1995120988

FEATURES AND APPLICATIONS OF THE GROOVE ANALYSIS PROGRAM (GAP)

Tu M. Nguyen
OAO Corporation
Lanham, Maryland

Jentung Ku
NASA Goddard Space Flight Center
Greenbelt, Maryland

and

Patrick J. Brennan
OAO Corporation
Lanham, Maryland

SUMMARY

An IBM Personal Computer (PC) version of the Groove Analysis Program (GAP) was developed to predict the steady state heat transport capability of an axially grooved heat pipe for a specified groove geometry and working fluid. In the model, the capillary limit is determined by the numerical solution of the differential equation for momentum conservation with the appropriate boundary conditions. This governing equation accounts for the hydrodynamic losses due to friction in liquid and vapor flows and due to liquid/vapor shear interaction. Back-pumping in both 0-g and 1-g is accounted for in the boundary condition at the condenser end. Slug formation in 0-g and puddle flow in 1-g are also considered in the model. At the user's discretion, the code will perform the analysis for various fluid inventories (undercharge, nominal charge, overcharge, or a fixed fluid charge) and heat pipe elevations. GAP will also calculate the minimum required heat pipe wall thickness for pressure containment at design temperatures that are greater than or lower than the critical temperature of the working fluid.

This paper discusses the theory behind the development of the GAP model. It also presents the many useful and powerful capabilities of the model. Furthermore, a correlation of flight test performance data and the predictions using GAP is presented and discussed.

NOMENCLATURE

A	Cross-sectional area
g	Gravitational constant
K	Permeability
N	Number of grooves
P	Pressure
Q	Axial heat flow
QL	Heat transport capability at capillary limit
R	Meniscus radius
Re	Reynolds number
R_i	Groove root radius
R_r	Groove root corner radius
R_t	Groove tip corner radius
R_v	Vapor core radius
T_s	Pseudo-land thickness
WP	Wetted perimeter
W_g	Groove width
x	Axial location
γ	Angle to define groove geometry in Figure 1
δ	Angle to define groove geometry in Figure 1

θ	Angle to define groove geometry in Figure 1
ξ	Groove land taper angle
θ_c	Contact angle
λ	Heat of vaporization
μ	Dynamic Viscosity
ν	Kinematic Viscosity
ϕ	Groove aspect ratio (half groove width/groove depth)
Ψ	Function defined in equation (5) or (6)
ρ	Density
ω	Angular velocity
σ	Surface tension

Subscripts

l	Liquid
v	Vapor
vl	Vapor/Liquid
x	Axial direction

ACRONYMS

ATS	Applications Technology Satellite
CRYOHP	Cryogenic Heat Pipe Experiment
GAP	Groove Analysis Program
HPP	Heat Pipe Performance Experiment
NASA	National Aeronautics and Space Administration
PC	Personal Computer
RPM	Revolutions Per Minute

INTRODUCTION

In recent years, spacecraft size and power requirements have increased, along with a corresponding demand for more efficient waste heat rejection. The design of heat pipe-based spacecraft thermal management systems requires a clear understanding of the thermal performance and working fluid behavior of heat pipes in microgravity. On Earth, the strong gravitational field dominates the capillary forces developed in the heat pipe wick. However, in the absence of gravity, the surface tension forces within the wick are the heat transport's limiting factor. One method of predicting 0-g performance is by extrapolating ground test data, but the presence of a liquid puddle in the condenser can make this technique unreliable. This is particularly true with axially grooved ammonia heat pipes at the high end of their operating temperature range and with most cryogenic fluids because of their low surface tensions.

The principal microgravity application of heat pipe technology is cooling electronics packages in spacecraft and satellites. Commercial telecommunication spacecraft alone are utilizing more than two thousand heat pipes annually for high power thermal management. The majority of these pipes are aluminum/ammonia axially grooved tubing because of their simplicity and high reliability. It has been very apparent that there is a need to accurately predict the microgravity performance characteristics of a heat pipe to minimize the penalties associated with over-design. One problem that often arises is how to use ground test data to predict microgravity thermal performance of a heat pipe. In space, the heat

pipes can also be exposed to a wide range of temperatures, and the expansion and contraction of the working fluid can lead to excess or insufficient fluid inventories. During a cold startup scenario, a heat pipe containing the correct fluid charge for nominal operating temperatures may be undercharged due to liquid contraction. One common method of preventing this condition is to overcharge the heat pipe by 5 percent or more. At higher operating temperatures this leads to excess fluid that could form a thick film over the condenser wick, or a liquid slug, either of which will result in decreased heat rejection efficiency and higher operating temperatures. Also, as a result of limited heat pipe performance flight data, thermal systems engineers currently must specify heat pipes with large performance margins to compensate for possible degradations and uncertainties in heat transport capacity, therein incurring volume and weight penalties.

Therefore, a design tool is needed to assist the thermal engineers in designing an axially grooved heat pipe for a particular space application. This design tool must be accurate in predicting the thermal performance of a heat pipe at any operating condition and also be easy to use. This IBM PC version of GAP was designed to accomplish both requirements.

MATHEMATICAL FORMULATION

An IBM PC version of the GAP model was developed to predict the steady state heat transport capacity of an axially grooved heat pipe for a specified groove geometry and working fluid. An example of the geometry applicable to GAP is the divergent groove shown in Figure 1. A full description of the model is contained in the user's manual (Reference 1).
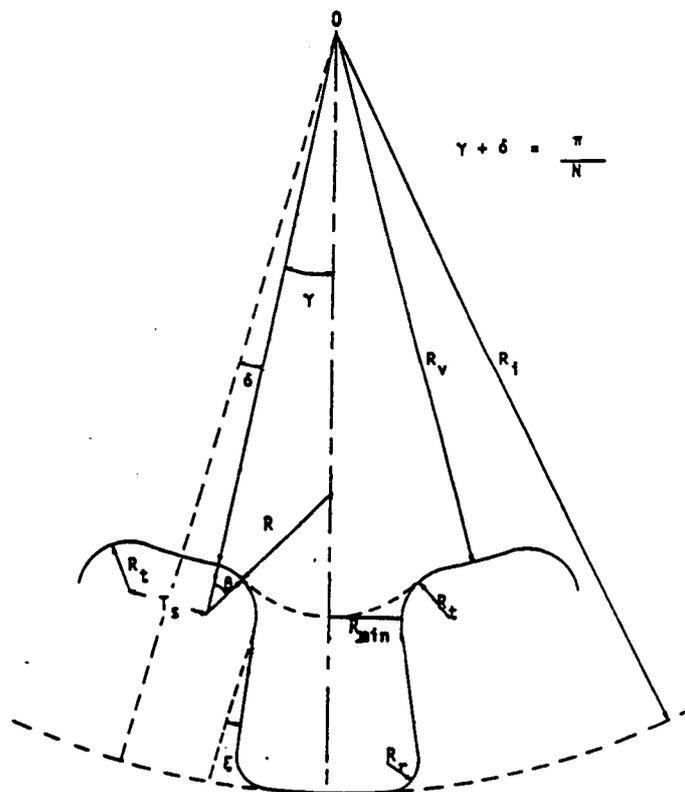

Figure 1. Divergent Groove Geometry

55

In the model, the capillary limit of the heat pipe is determined by the numerical solution of the differential equation for momentum conservation with the appropriate boundary conditions. This governing equation accounts for the hydrodynamic losses due to friction in the liquid and vapor flows and due to liquid/vapor shear interaction. Back-pumping which is the capillary force that develops at the condenser end in both 1-g and 0-g is accounted for in the condenser boundary condition. Slug formation in 0-g and puddle flow in 1-g are also considered in the model. At the user's discretion, the code will perform the analysis for various heat pipe elevations and fluid inventories, including both undercharged and overcharged conditions. GAP will also calculate the minimum heat pipe wall thickness required for pressure containment at design temperatures that are greater than or lower than the critical temperature of the working fluid.

The capillary pumping limit is the transport limit generally experienced in 0-g heat pipe operation. Sonic and vapor limits are typically encountered in 1-g applications with very high axial heat fluxes or when operating near the melting point. The viscous limit becomes important if the pipe is very long and is operated at lower temperature range of the working fluid. The capillary limit occurs when the capillary pumping head can no longer sustain the hydrodynamic losses. In the operation of an axial groove heat pipe, as heat is applied to the evaporator and is removed from the condenser, fluid flows develop within the heat pipe. The vapor flows to the condenser end and the liquid in the grooves is pumped back to the evaporator. In addition to the viscous pressure drops due to the vapor and liquid flows, there is an additional pressure drop due to shearing at the liquid/vapor interface. For steady state operation, the sum of all these pressure drops and those of body forces must be balanced by the capillary pumping force developed by the groove opening, i.e.

$$\Delta P_{x,capillary} = \Delta P_{x,v} + \Delta P_{x,l} + \Delta P_{x,vl} + \sum \Delta P_{x,body} \qquad (1)$$

This constitutes the basic hydrodynamic governing equation for an axially grooved heat pipe. A differential form of this equation can be derived by making the following assumptions:

(1) One dimensional laminar liquid flows in the axial groove and one dimensional laminar or turbulent vapor flow in the inner core of the heat pipe;

(2) The groove depth is small compared to its wicking height, thus the hydrostatic loss associated with the groove depth is negligible;

(3) Identical grooves with uniform groove properties for each groove over the entire length; and

(4) Uniform heat transfer in the evaporator and condenser.

The governing equations are thus:

- Laminar vapor flow ($Re_v < 2000$)

$$\frac{\sigma Cos\theta_c}{R^2} \frac{dR}{dx} = \rho_l gSin\beta + \left[\frac{8\mu_v}{\rho_v A_v R_v^2} + \frac{\mu_l}{KA_l \rho_l} \left(1 + \frac{\phi^2}{3} \psi_x \right) \right] \frac{Q(x)}{\lambda} \qquad (2)$$

- Turbulent vapor flow ($Re_v > 2000$)

$$\frac{\sigma Cos\theta_c}{R^2} \frac{dR}{dx} = \rho_l g Sin\beta + \frac{0.06558\mu_v^{0.25}}{\rho_v A_v^{1.75} R_v^{1.25}} \left(\frac{Q(x)}{\lambda}\right)^{1.75} + \frac{\mu_l}{KA_l\rho_l}\left(1+\frac{\phi^2}{3}\psi_x\right)\frac{Q(x)}{\lambda} \quad (3)$$

where the groove aspect ratio ϕ, defined as the ratio of half the groove width to the groove depth, can be written as

$$\phi = \frac{(R_v+R_t) Sin\gamma - R_t}{R_i-R_v} \quad (4)$$

and the parameter ψ_x which accounts for liquid/vapor shear (Reference 2) is defined as

- Laminar vapor flow

$$\psi_x = \frac{4(R_i-R_v)}{R_v} \frac{v_v}{v_l} \frac{A_{l,x}}{A_v} \quad (5)$$

- Turbulent vapor flow

$$\psi_x = 0.03279 \frac{R_i-R_v}{R_v^{0.25}} \frac{A_{l,x}}{A_v^{1.75}} \frac{\mu_v^{0.25}}{\rho_v v_l} \left(\frac{Q(x)}{\lambda}\right)^{0.75} \quad (6)$$

The left hand side of equation (2) or (3) represents the capillary pumping. The right hand side represents the following pressure losses:

(1) The first term is the hydrostatic loss;
(2) The second term is the viscous vapor loss; and
(3) The third term is the liquid flow loss which combines both the viscous loss and the liquid/vapor shear interaction. The magnitude of the shear loss relative to the viscous liquid loss is $\phi^2\psi_x/3$. The factor 1/3 in this term is recommended in Reference 3 for grooves that have groove depths larger than groove widths, which is usually the case for axially grooved heat pipes.

Equations (2) and (3) are solved by using a fourth order Runge-Kutta integration method. The variables include working fluid properties, axial groove geometries, and heat pipe dimensions. The boundary conditions and heat distribution are also required to completely specify the problem. The integration of expression (2) or (3) yields the local meniscus radius required to support the local pressure drop in each groove. The integration process starts from the evaporator end with a minimum meniscus radius specified as half the groove width and proceeds to the condenser end. This process is normally repeated many times with the heat transport rate continuously updated until the boundary condition at the condenser end is satisfied. The liquid flow analysis conducted in Reference 2 demonstrated that the maximum transport is obtained when the meniscus radius at the upstream end of the evaporator is a minimum. Therefore, the boundary condition at the evaporator end for both 0-g and 1-g environments

for all fluid charge conditions is

$$@ \; x = 0 \qquad R = R_{min} = \frac{W_g}{2} \qquad (7)$$

where R_{min} for the axial groove geometry is shown in Figure 1.

At the condenser end, e.g. x = L, the boundary condition depends on the fluid charge condition and the gravitational environment. For nominal charge and overcharge, the meniscus radius is set to a maximum value to obtain the highest capillary pumping in the grooves. In 0-g, the excess liquid will form a slug in the vapor core at the condenser end. Two radii of curvature both equal to half the vapor core diameter define the minimum energy condition at the slug's liquid/vapor interface. Mass continuity between the liquid slug and the liquid in the grooves in turn dictates an equivalent groove radius in the condenser. In the code, the meniscus radius at the condenser end is set at half the vapor core radius to model this condition

$$For \; 0\text{-}g, \quad @ \; x = L \qquad R = R_{max} = \frac{R_v}{2} \qquad (8)$$

In 1-g, when there is excess liquid in the pipe, a puddle will form at the condenser end. Beyond the puddle, if preferential drainage is neglected, only one radius of curvature exists in the groove. This liquid/vapor interface extends from the tip of one fin to the tip of the adjacent fin and its maximum value is equal to the vapor core radius, i.e.

$$For \; 1\text{-}g, \quad @ \; x = L \qquad R = R_{max} = R_v \qquad (9)$$

For undercharge condition, the meniscus radius at the condenser end is incremented gradually from R_{min} up to R_{max} until the specified fluid charge is found. Thus, depending on the amount of undercharge and the gravitational environment, the actual meniscus radius at the condenser end will be between R_{min} and the value shown in equation (8) or (9).

The program estimates the maximum transport using a closed form solution for liquid losses only. It then uses an incremental heat load based on this value and solves the differential equation to determine the axial variation of the meniscus. Once this is known, the corresponding liquid and vapor inventories are calculated. Repeating this solution procedure will then yield the maximum transport that can be obtained as a function of fluid inventory up to the nominal charge condition.

FEATURES IN GAP

The IBM PC version of this GAP code is a menu-driven computer program designed for user friendliness and flexibility not only in the data input but also in the code operation and in the processing of the output data. The general flow chart of the code is shown in Figure 2. The code is written in standard FORTRAN 77 and assembly language. It is designed to operate with an IBM PC or compatible system that employs an 80286, 80386, or 80486 microprocessor with an appropriate coprocessor. The present code has been intended to be interactive and user-friendly. It can be installed into a PC in a few minutes and with the interactive data input feature, the user can run the code immediately to get the results. Other special features of the code include:

- Multiple runs for various heat pipe elevations and over a wide range of temperatures are readily achieved;
- A comprehensive data base that contains the properties of 24 heat pipe working fluids is included with the code. A listing of these working fluids and their corresponding range of operating temperatures are included in Table 1;
- For pressure containment, the minimum required heat pipe wall thickness can be determined for specified factors of safety; and
- At the user's discretion, the desired output data is written to a plot file which can be imported to most spreadsheet or graphic software programs for fast quality plotting.
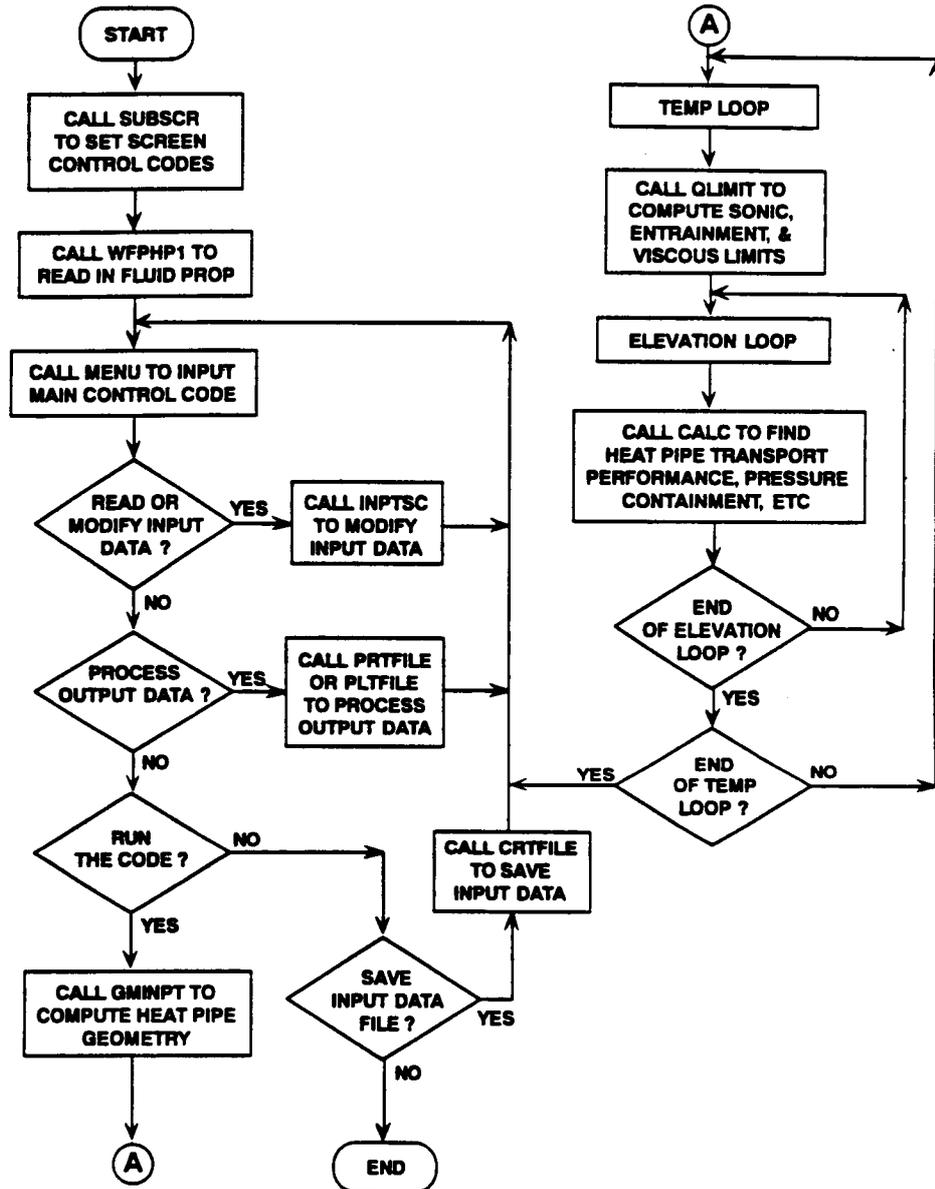

Figure 2. GAP General Flowchart

59

Table 1. Heat Pipe Working Fluids in GAP

Working Fluid	Temperature Range (K)	Working Fluid	Temperature Range (K)
Acetone	250 to 474	Freon 21	213 to 449
Ammonia	200 to 404	Freon 113	293 to 368
Argon	85 to 149	Heptane	273 to 472
Benzene	270 to 559	Lithium	500 to 2099
Butane	260 to 349	Mercury	280 to 1069
Cesium	400 to 1499	Methane	91 to 189
Dowtherm-A	373 to 669	Methanol	273 to 502
Dowtherm-E	283 to 609	Nitrogen	65 to 124
Ethane	100 to 304	Oxygen	55 to 154
Freon 11	293 to 412	Potassium	400 to 1799
Freon 13	163 to 292	Sodium	400 to 1499
Freon 14	130 to 221	Water	273 to 642

FLIGHT DATA CORRELATIONS

The GAP code was used to predict the heat transport capacity of the axially grooved heat pipes employed in the Heat Pipe Performance (HPP) (References 4 and 5) and the Cryogenic Heat Pipe (CRYOHP) (Reference 6) flight experiments. The results were obtained by running the code to predict 0-g performance for each pipe with a nominal charge at various operating temperatures. These results were then correlated with the flight test data to assess the accuracy of the code. The following sections discuss the GAP predicted performance and the associated correlations with flight data for these pipes.
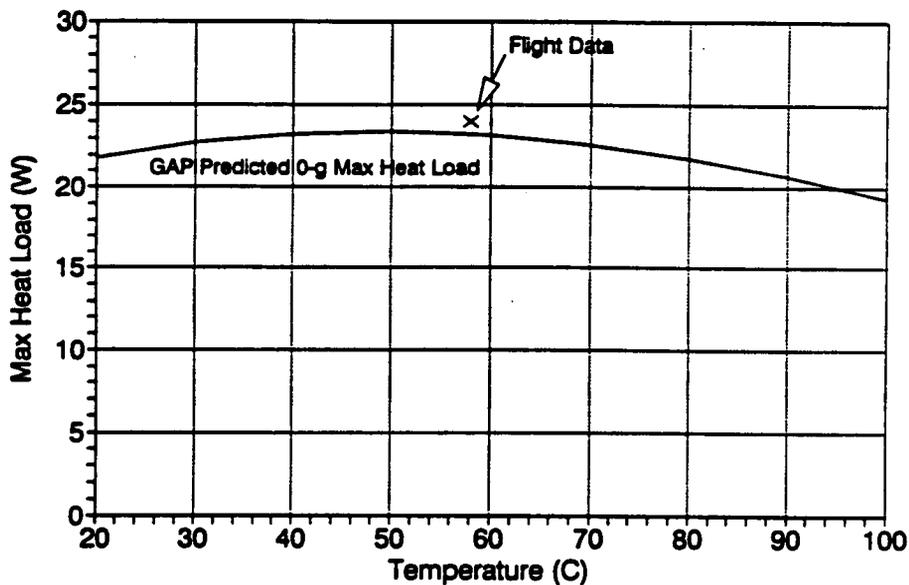
HPP Freon 113/Aluminum Heat Pipe

This heat pipe utilizes a rectangular groove geometry with its measured groove geometry shown in Table 2. The detail of the HPP experiment design is discussed in References 4 and 5. The GAP predicted 0-g steady state heat transport capacity of the pipe as a function of the operating temperature range of interest is shown in Figure 3. At 58°C, the pipe is expected to transport about 23 watts before dry-out occurs. This power level is in excellent agreement with the actual 24 watts obtained in flight. It should be noted that these pipes were charged for operation at 40°C and have a 4.9% overcharge at 58°C. This charge is based on the accounting for meniscus recession.

The prediction of the heat transport capacity of a heat pipe subjected to adverse spin was determined in the following manner. First, the maximum transport under a no spin condition was obtained from GAP. Then, this value was used in the following expression to determine the heat transport capacity of a heat pipe under adverse spin as:

$$QL = (QL)_{max} \left[1 - \frac{1}{4} \frac{\rho_l}{\sigma} \frac{W_g}{} \omega^2 \left(R_c^2 - R_e^2 \right) \right] \tag{10}$$

Table 2. HPP Freon 113/Aluminum Heat Pipe Design Summary

Groove Cross Section	Rectangular Form
Number of Grooves	40
Outer Diameter (inch, mm)	0.499, 12.675
Inner Diameter (inch, mm)	0.437, 11.10
Vapor Core Diameter (inch, mm)	0.364, 9.246
Fin Tip Corner Radius (inch, mm)	0.00428, 0.1087
Groove Root Corner Radius (inch, mm)	0.00409, 0.1039
Pseudo-land Tip Thickness (inch, mm)	0.00638, 0.1621
Groove Land Taper Angle (radian)	0.047
Groove Width (inch, mm)	0.0143, 0.3635
Wetted Perimeter (1 Groove) (inch, mm)	0.0909, 2.308
Total Groove Area (inch², mm²)	0.0222, 14.31
Evaporator Length (inch, mm)	4.0, 101.6
Transport Section Length (inch, mm)	0.0, 0.0
Condenser Length (inch, mm)	12.76, 324.1

$D_o = 12.68$ mm $D_i = 11.1$ mm $D_v = 9.246$ mm   40 Grooves
$W_g = 0.3635$ mm   WP = 2.308 mm $R_t = 0.1087$ mm $A_g = 14.31$ mm^2

Figure 3. HPP Freon Heat Pipe 0-g Transport Capability vs. Temperature

61

where QL = transport capacity of the heat pipe experiencing adverse spin
  $(QL)_{max}$ = maximum transport capacity under no spin condition
  ρ_l = density of the liquid phase
  ω = angular velocity
  σ = surface tension
  R_c = linear distance from the center of rotation to the end of the condenser section
  R_e = linear distance from the center of rotation to the end of the evaporator section
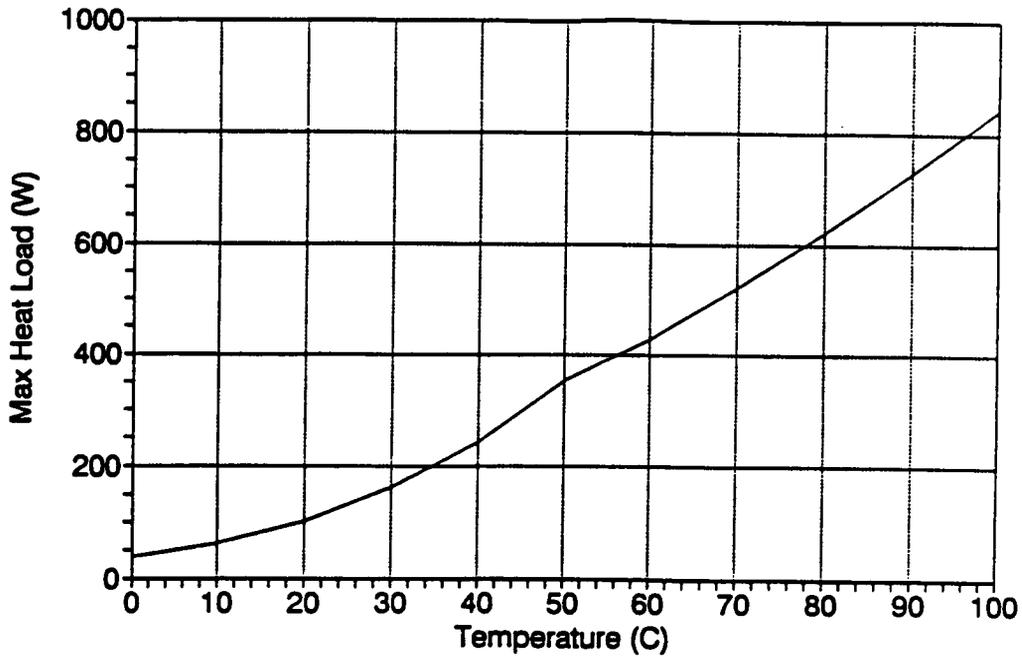 W_g = groove width

With this procedure, the maximum heat load for the pipe at 32°C versus adverse spin rate is computed. The data indicates that at a spin rate of about 6 RPM, the pipe can transport a maximum power of 6 watts. This result is in good agreement with the flight data which showed that dry-out for the pipe occurred between 6 and 8 RPM with 6 watts applied.

HPP Water/Copper Heat Pipe

This heat pipe utilizes a rectangular groove geometry. Table 3 provides the groove measurement of this pipe. The GAP code was used to predict the 0-g steady state heat transport capacity of the pipe as a function of the operating temperature range as shown in Figure 4. Note that at 50°C, the curve seems to have a discontinuity. This is the point at which the vapor flow in the pipe is predicted to transition from a laminar to a turbulent flow regime. The pressure losses due to vapor flow and vapor-liquid shear in turbulent flow are higher than those in laminar flow; and thus, the slope of the heat transport curve decreases slightly. With the same procedure used for the freon heat pipe, the heat transport capacity of this water heat pipe at 72°C was predicted as a function of adverse spin and it is shown in Figure 5. From this Figure, one would expect a pipe transporting about 40 watts to dry out at about 10.4 RPM. This turns out to be the case in flight where the measured dry-outs were obtained between 10 to 12 RPM.

Table 3. HPP Water/Copper Heat Pipe Design Summary

Groove Cross Section	Rectangular Form
Number of Grooves	25
Outer Diameter (inch, mm)	0.497, 12.631
Inner Diameter (inch, mm)	0.454, 11.521
Vapor Core Diameter (inch, mm)	0.375, 9.535
Fin Tip Corner Radius (inch, mm)	0.00464, 0.1178
Groove Root Corner Radius (inch, mm)	0.01462, 0.3713
Pseudo-land Tip Thickness (inch, mm)	0.00391, 0.09934
Groove Land Taper Angle (radian)	0.08155
Groove Width (inch, mm)	0.0351, 0.8915
Wetted Perimeter (1 Groove) (inch, mm)	0.1092, 2.775
Total Groove Area (inch², mm²)	0.0335, 21.622
Evaporator Length (inch, mm)	4.0, 101.6
Transport Section Length (inch, mm)	0.0, 0.0
Condenser Length (inch, mm)	12.76, 324.1

Do = 12.63 mm   Di = 11.52 mm   Dv = 9.535 mm   25 Grooves
Wg = 0.8915 mm   WP = 2.775 mm   Rt = 0.1178 mm   Ag = 21.62 mm^2

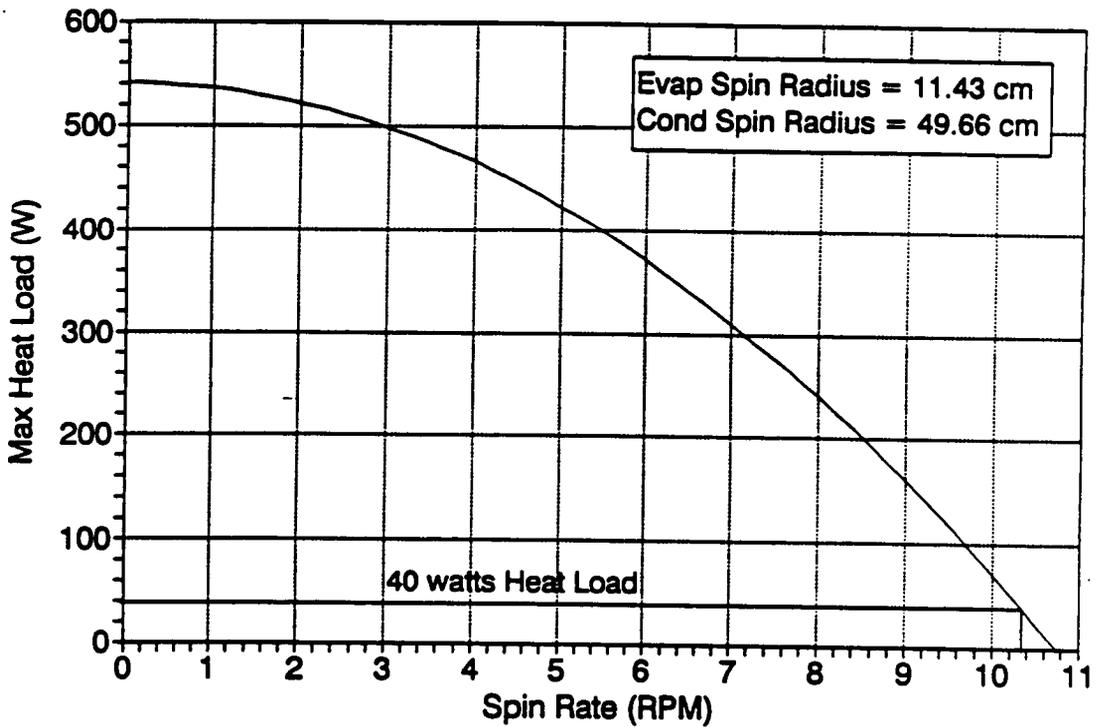*Figure 4. HPP Water Heat Pipe 0-g Transport Capability vs. Temperature*

Evap Spin Radius = 11.43 cm
Cond Spin Radius = 49.66 cm

40 watts Heat Load

Figure 5. HPP Water Heat Pipe 0-g Transport @ 72°C vs. Adverse Spin Rate
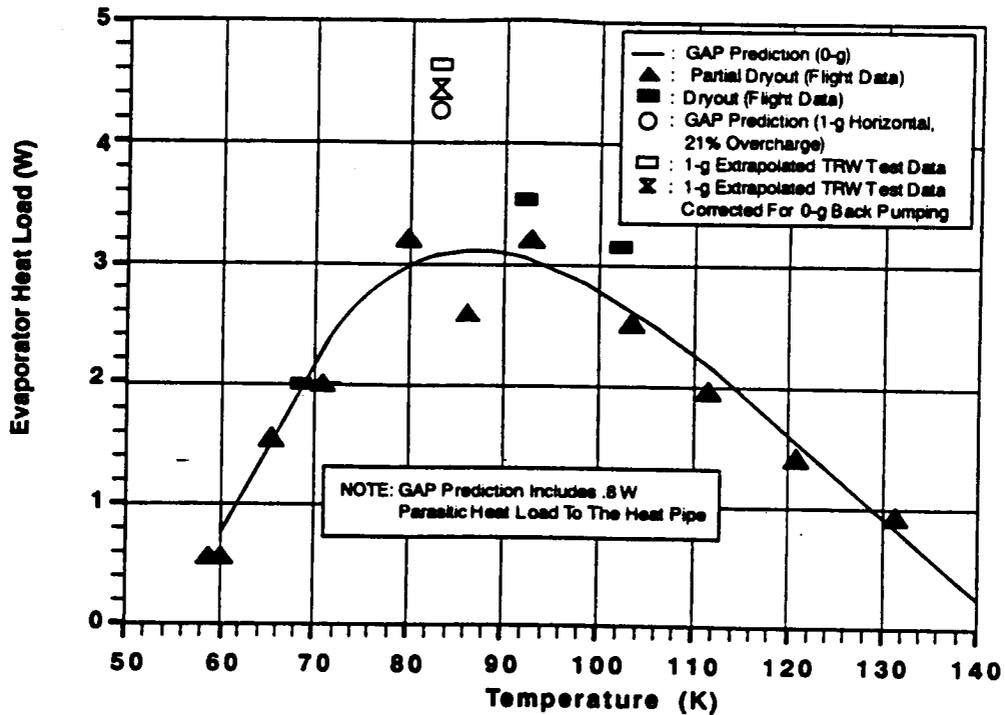
63

TRW Cryogenic Heat Pipe (CRYOHP)

This heat pipe has oxygen working fluid and employs a rectangular groove geometry with relatively shallow grooves (~ 0.8 mm deep) as shown in Table 4. This design was intentionally degraded so that its heat transport capacity could be tested within the limits of the CRYOHP's cooling capacity (~ 5 watts at 80 K). The CRYOHP experiment design and component test results are discussed in Reference 7.

The 0-g steady state heat transport capacity of the heat pipe predicted by GAP is shown in Figure 6 with the flight and ground test data. Flight data points are the actual electrical heater power applied to the evaporator. The GAP predictions include a 0.8 watt parasitic heat leak from the surrounding environment to the heat pipe. This heat leak was determined from ground and flight data transients (Reference 6). The GAP predictions are in good agreement with the flight test data. GAP correctly predicted the fully dry-out heat load at 69 K and under-predicted the values at 92 K and 102 K by approximately 0.5 watt. The applied power increments for the TRW pipe are 0.5 watt and therefore there is up to a 0.5 watt uncertainty when full dry-out occurs.

Also shown in Figure 6 is the 1-g performance at 82 K that was extrapolated from the component tilt test results presented in Reference 7. At this temperature, the pipe was predicted to be over-filled as listed in Table 5. The nominal charge required at 82 K as predicted by GAP is 8.54 grams. If the grooves were filled without any meniscus recession, the charge would increase by 1.05 grams or 12.2% above the nominal charge with recession. In addition to the amount associated with meniscus recession and based on the actual 10.3 grams charge, there is an additional 0.71 gram or 8.4% of further overcharge at 82 K. The 0-g slug length at 82 K for this overcharge condition is 3.63 cm. The GAP predicted performance at 82 K for a 1-g horizontal test condition was obtained with this overcharge (i.e. 1.76 grams excess) and is plotted in Figure 6. Note that in this 1-g analysis, the same 0.8 watt parasitic heat leak to the pipe was assumed. This theoretical data point is only 0.3 watt lower than the extrapolated ground-test data point.

Table 4. TRW CRYOHP Heat Pipe Design Summary

Groove Cross Section	Rectangular Form
Number of Grooves	17
Outer Diameter (inch, mm)	0.442, 11.224
Inner Diameter (inch, mm)	0.349, 8.872
Vapor Core Diameter (inch, mm)	0.2865, 7.277
Fin Tip Corner Radius (inch, mm)	0.004, 0.1016
Groove Root Corner Radius (inch, mm)	0.00508, 0.1291
Pseudo-land Tip Thickness (inch, mm)	0.02887, 0.7334
Groove Land Taper Angle (radian)	0.1685
Groove Width (inch, mm)	0.0175, 0.445
Wetted Perimeter (1 Groove) (inch, mm)	0.0822, 2.089
Total Groove Area (inch², mm²)	0.0094, 6.065
Evaporator Length (inch, mm)	6.0, 152.4
Transport Section Length (inch, mm)	40.8, 1015.24
Condenser Length (inch, mm)	6.0, 152.4
Fluid Charge (gr)	10.3

"AS-FABRICATED" GROOVE DIMENSIONS FOR GAP PREDICTIONS:
D_O = 11.22 mm D_I = 8.872 mm D_V = 7.277 mm   17 Grooves
W_g = 0.445 mm   WP = 2.089 mm R_t = 0.1016 mm A_g = 6.065 mm^2

Figure 6. TRW CRYOHP Heat Pipe Transport Capability vs. Temperature

Table 5. TRW CRYOHP Heat Pipe Fluid Charge Conditions
Actual Charge = 10.3 gr

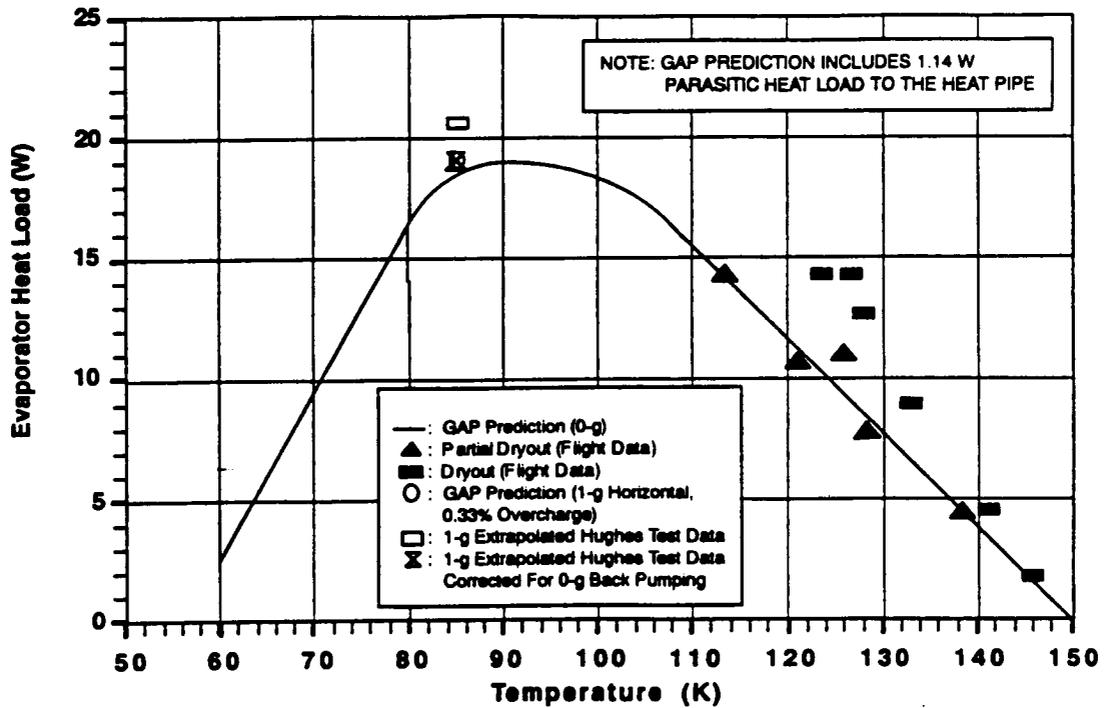| Operating Temperature (K)	GAP Computed Nominal Charge (gr)	Percentage Charge (Actual/GAP Nominal)
60	8.93	115.34
70	8.71	118.23
80	8.58	120.11
90	8.40	122.62
100	8.29	124.24
110	8.45	121.89
120	9.05	113.86
130	10.16	101.36
140	12.17	84.61
150	18.06	57.02

Hughes Aircraft Cryogenic Heat Pipe (CRYOHP)

This heat pipe also utilizes oxygen with the conventional ATS rectangular groove geometry (Reference 8). Design details of the heat pipe and the groove geometry obtained from a shadowgraph measurement are listed in Table 6. The oxygen charge for this heat pipe is 33.7 grams.

The GAP predicted 0-g steady state transport capability of this heat pipe is shown in Figure 7 versus operating temperature. Flight and thermal vacuum test data are also included in this figure. The GAP predictions include a 1.1 watt uniform parasitic heat leak to the heat pipe from the surroundings (Reference 6). In general, the flight data is in good agreement with the GAP prediction. A partial dry-out is the best measure of a heat pipe's capillary transport limit and these data points correlate almost exactly over the test temperature range of 100 to 140 K. The model tends to under-predict the dry-out condition by almost 5 watts at 128 K. This data point was obtained under transient condition because of inadequate cooling, and transient performance is not an accurate measure of the transport limit.

Also shown in Figure 7 is the 1-g performance at 85 K that was extrapolated from the component tilt tests in Reference 8. At this temperature, the Hughes heat pipe was predicted to be slightly over-filled by just 0.1 gram. Fluid charge conditions at other temperatures were predicted by GAP and are listed in Table 7. Again the performance of this heat pipe at 85 K for a 1-g horizontal position with a 1.14 watt parasitic heat leak to the pipe was predicted and is included in Figure 7. This single GAP data point is approximately 1.5 watts lower than the extrapolated ground-test data. The small difference is, however, well within the accuracy of the groove measurements and the experimental error.

Table 6. Hughes Aircraft CRYOHP Heat Pipe Design Summary

Groove Cross Section	Rectangular Form
Number of Grooves	27
Outer Diameter (inch, mm)	0.627, 15.914
Inner Diameter (inch, mm)	0.429, 10.897
Vapor Core Diameter (inch, mm)	0.334, 8.484
Fin Tip Corner Radius (inch, mm)	0.0064, 0.1623
Groove Root Corner Radius (inch, mm)	0.00625, 0.1588
Pseudo-land Tip Thickness (inch, mm)	0.00159, 0.0403
Groove Land Taper Angle (radian)	0.0546
Groove Width (inch, mm)	0.0259, 0.658
Wetted Perimeter (1 Groove) (inch, mm)	0.1281, 3.253
Total Groove Area (inch^2, mm^2)	0.036, 23.226
Evaporator Length (inch, mm)	6.0, 152.4
Transport Section Length (inch, mm)	42.8, 1065.2
Condenser Length (inch, mm)	6.0, 152.4

NOTE: GAP PREDICTION INCLUDES 1.14 W
PARASITIC HEAT LOAD TO THE HEAT PIPE

Legend:
—— : GAP Prediction (0-g)
▲ : Partial Dryout (Flight Data)
■ : Dryout (Flight Data)
O : GAP Prediction (1-g Horizontal, 0.33% Overcharge)
□ : 1-g Extrapolated Hughes Test Data
⊠ : 1-g Extrapolated Hughes Test Data Corrected For 0-g Back Pumping

"AS-FABRICATED" GROOVE DIMENSIONS FOR GAP PREDICTIONS:

D_O = 15.91 mm D_I = 10.90 mm D_V = 8.487 mm   27 Grooves

W_g = 0.658 mm   WP = 3.253 mm R_t = 0.1623 mm A_g = 23.23 mm^2

Figure 7. Hughes Aircraft CRYOHP Heat Pipe Transport Capability vs. Temperature

Table 7. Hughes Aircraft CRYOHP Heat Pipe Fluid Charge Conditions
Actual Charge = 33.7 gr

Operating Temperature (K)	GAP Computed Nominal Charge (gr)	Percentage Charge (Actual/GAP Nominal)
60	35.69	94.42
70	34.78	96.89
80	33.79	99.73
90	32.99	102.15
100	31.68	106.38
110	30.73	109.66
120	30.57	110.24
130	31.20	108.01
140	32.39	104.04
150	36.66	91.93

CONCLUSIONS

An IBM PC model of GAP was developed to predict the steady state thermal performance of an axially grooved heat pipe operating in 1-g or microgravity environment. The model is user-friendly and easy to use. It has been shown to accurately predict the transport capability of axially grooved heat pipes. For the HPP flight experiment, static dryout limits of the aluminum/freon pipes in microgravity were obtained and are in excellent agreement with the analytical predictions by the model. The transport limits of the freon and water pipes under adverse spin also correlate well with the predictions by the GAP model. For further verification, the computer model was applied to predict the transport limits of two aluminum/oxygen pipes flown in the CRYOHP experiment. These predictions are also in excellent agreement with the test data over a wide range of operating temperatures.

In support of the on-going Heat Pipe Performance Reflight (HPP-2) project and with the recommendations by several users, the current GAP model is being upgraded to accommodate the actual boundary conditions of an axially grooved heat pipe utilized in most applications. The following features have been planned for this new version:

- Boiling limit will be included in the calculation of transport limits. Heat diffusion in the heat pipe wall will be accounted for in this calculation. Therefore, thermal conductivity of the heat pipe wall is an important parameter and will be correlated with the evaporator temperature;
- Asymmetric heating and cooling of the evaporator and condenser, respectively, will be considered in the computation of maximum heat transport capability. In most practical applications, the heat pipe is embedded inside a panel, which results in non-uniform heating or cooling of the evaporator or condenser, respectively. In these cases, the heat pipe exhibit lower heat transport capability because of local dry-out in the grooves; and
- Multiple sections of evaporator, transport, and condenser will also be included in the model. This feature is critical to account for distributed heat loads along a heat pipe in many applications.

REFERENCES

1. Nguyen, T. M., "User's Manual for Groove Analysis Program (GAP) IBM PC Version 1.0," OAO Corporation, February 1994.
2. Kroliczek, E. J. and Jen, H., "Axially Grooved Heat Pipe Study," Summary Report, BK012-1009, B&K Engineering, Incorporated, June 1977.
3. Hufschmidt, E. et al. "The Shearing Effect of Vapor Flow on Laminar Liquid Flow in Capillaries of Heat Pipe," NASA TT-F-16601, October 1975.
4. Heat Pipe Performance Experiment (HPP) Final Report, Fleishman, G. L. and Grier, K. D., Hughes Aircraft Company, Electron Dynamics Division, June 1993.
5. Buchko, M. T., Brennan, P. J., and Nguyen, T. M., "Flight and Ground Test Data Analysis for the Heat Pipe Performance (HPP) Experiment," SAE Paper Number 941300, June 1994.
6. Brennan, P. J., Thienel, L., Swanson, T., and Morgan, M., "Flight Data for the Cryogenic Heat Pipe (CRYOHP) Experiment," AIAA Paper Number 93-2735, July 1993.
7. Antoniuk, D. and Pohner, J., "Development of an Oxygen Axial Groove Heat Pipe for A Microgravity Flight Experiment," AIAA Paper Number 91-1357, June 1991.
8. Fleishman, G. L., Chiang, T. C., and Ruff, R. D., "Oxygen Heat Pipe 0-g Performance Evaluation Based on 1-g Tests," AIAA Paper Number 91-1358, June 1991.